



Exacta

ISSN: 1678-5428

exacta@uninove.br

Universidade Nove de Julho

Brasil

Henriques Librantz, André Felipe; Gomes, Laércio; Gomes Tarelho, Luiz Vicente; Ranieri, Izilda  
Márcia

Investigation of energy shift of 4f3 and 4f5d levels in Nd-doped YLF and LLF crystals

Exacta, vol. 4, núm. 1, janeiro-junho, 2006, pp. 123-128

Universidade Nove de Julho

São Paulo, Brasil

Available in: <http://www.redalyc.org/articulo.oa?id=81040112>

- How to cite
- Complete issue
- More information about this article
- Journal's homepage in redalyc.org

redalyc.org

Scientific Information System

Network of Scientific Journals from Latin America, the Caribbean, Spain and Portugal

Non-profit academic project, developed under the open access initiative

# Investigation of energy shift of $4f^3$ and $4f^25d$ levels in Nd-doped YLF and LLF crystals <sup>1 2</sup>

André Felipe Henriques Librantz

Doutor em Tecnologia Nuclear [Materiais] – Ipen;  
Pesquisador-colaborador – Cnen/Ipen;  
Professor na graduação [Ciência da Computação] – Uninove.  
librantz@ipen.br, São Paulo – SP [Brasil]

Laércio Gomes

Doutor em Tecnologia Nuclear [Materiais] – Ipen;  
Pesquisador-colaborador – Cnen/Ipen.  
lgomes@ipen.br, São Paulo – SP [Brasil]

Luiz Vicente Gomes Tarelho

Doutor em Tecnologia Nuclear [Materiais] – Ipen;  
Pesquisador-colaborador – Cnen/Ipen.  
ltarelho@ipen.br, São Paulo – SP [Brasil]

Izilda Márcia Ranieri

Doutora em Tecnologia Nuclear [Materiais] – Ipen;  
Pesquisadora-colaboradora – Cnen/Ipen.  
iranieri@ipen.br, São Paulo – SP [Brasil]

We observed ultraviolet (UV) luminescence from  $4f^25d$  and  $4f^3$  configuration in Nd-doped  $YLiF_4$  (YLF) and  $LuLiF_4$  (LLF) crystals induced by multiphotonic excitation of the three photons (532 nanometers [nm]). The LLF lattice is more compact than the YLF crystal and favours an absorption and emission shift of the main peaks due to crystal field strength. The red and blue shifts of the emission bands towards to lower (and higher) energy are different for the transitions from  $4f^3$  and  $4f^25d$  levels. The  $4f^3$  transitions have smaller shift (~5 times smaller than the shift of the  $4f^25d$ ) due to  $5s^25p^6$  closed-shell shielding effect. On the other hand the  $4f^25d$  transitions are more susceptible to lattice change. The effect of the crystalline field was compared for both lattice. The result shows that these emission bands from  $4f^25d$  configuration always shift to lower energy when substituting the  $Y^{3+}$  by  $Lu^{3+}$  (i.e., the last one has the ionic radius 5% smaller than  $Y^{3+}$ ).

**Key words:** Energy shift. LLF crystal. Ultraviolet.  
UV emission. YLF crystal.



## 1 Introduction

Rare earth ( $3^+$ )-doped crystals are very useful laser media for generating laser radiation in the visible and infrared region, based on transitions within the  $4f^{n-1}$  configuration. On the other hand, transitions based on  $4f^{n-1}5d$  are not much exploited. In spite of this, laser action in blue, UV and vacuum ultraviolet (VUV) have been demonstrated in  $Ce^{3+}$ , Er, Tm and  $Nd^{3+}$  in  $YLiF_4$  (YLF) and  $LuLiF_4$  (LLF) and other fluoride crystals (EHRlich; MOULTON; OSGOOD JUNIOR, 1979; CEFALAS et al., 1993; MAKHOV et al., 2000; JOUBERT et al., 2001; GUYOT; GUY; JOUBERT, 2001) and for a new fluoride system  $NaF-(Er, Y)F_3$  (KARIMOV et al., 2001). Solid-state materials doped with  $Nd^{3+}$  are very promising for using as laser medium emitting in the UV region (THOGERSEN; GILL; HAUGEN, 1996). The excitation can be performed directly to the level of interest or sequentially pumped. The most interesting pumping mechanism is the three steps excitations at 532 nm which has the advantage to match the second harmonic of Nd:YAG laser which is one of the most disseminated laser for optical pumping systems (THOGERSEN; GILL; HAUGEN, 1996; VENIKOUAS et al., 1984). The  $4f^n \rightarrow 4f^{n-1}5d$  transitions are characterized by a strong environmental interaction and they are responsible for the high oscillator strength and broadband absorption and emission spectra in the UV range. Otherwise, the intraconfigurational  $4f^n \rightarrow 4f^n$  transitions are parity forbidden and they are sharp and weak because they take place mostly by the forced electric dipole radiation induced by odd terms of the local crystal field (KOLLIA et al., 1998; POWELL, 1998<sup>4</sup>).

The spectrum characterization of the  $4f^3 \rightarrow 4f^25d$  and  $4f^3 \rightarrow 4f^3$  transitions provides information about the local level structure and electron-phonon coupling differences between  $4f^3$  and the

$4f^25d$  configurations because the crystal field perturbation is stronger for electrons in the 5d level than for those in the 4f level (POWELL, 1998<sup>4</sup>). This results in broad transition bands with a large Stokes shift and a higher probability for phonon-assisted transitions.

## 2 Experimental setup

Single crystals doped with neodymium were grown by the Czochralski technique under a purified argon atmosphere (WEGH; MEIJERINK; LAMMINMAKI, 2000). The starting growth material was doped with 3 mol% of Nd. The Nd concentration of 1.3 mol% was determined in the used samples by x-ray fluorescence technique. The YLF and LLF samples were cut and polished properly with the c-axis parallel to the longest side of the rectangular samples. The absorption spectra were performed using a Cary-Olis double-beam spectrophotometer interfaced to a computer. Using a time resolved spectroscopy system of 20 nanoseconds (ns) of resolution provided the emission spectra and the decay time determination. The laser pumping system consists of a frequency doubled Nd:YAG pulsed laser whose beam intensity is reduced and focused in the samples. The emission of the samples is focused into the monochromator that disperses and directs the light to the EMI S-20 photomultiplier tube. The detection system is connected to the 200 megahertz (MHz) Tektronix oscilloscope and a boxcar gated integrator coupled to a microcomputer.

In order to control the laser excitation energy at 532 nm, we use an injection telescope which firstly expands the laser beam by factor of four and then cut off most of the beam using an iris with a 2 millimeters (mm) aperture and focused to the sample by a convergent lens with focus of 300 mm. With this set arrangement it is

possible to have a reduction in the pulse energy by a factor of 100. The reduction of the laser energy to hundred of microjoules ( $\mu\text{J}$ ) was necessary to avoid the self focusing in the  $\mu\text{J}$  range, destroying the samples.

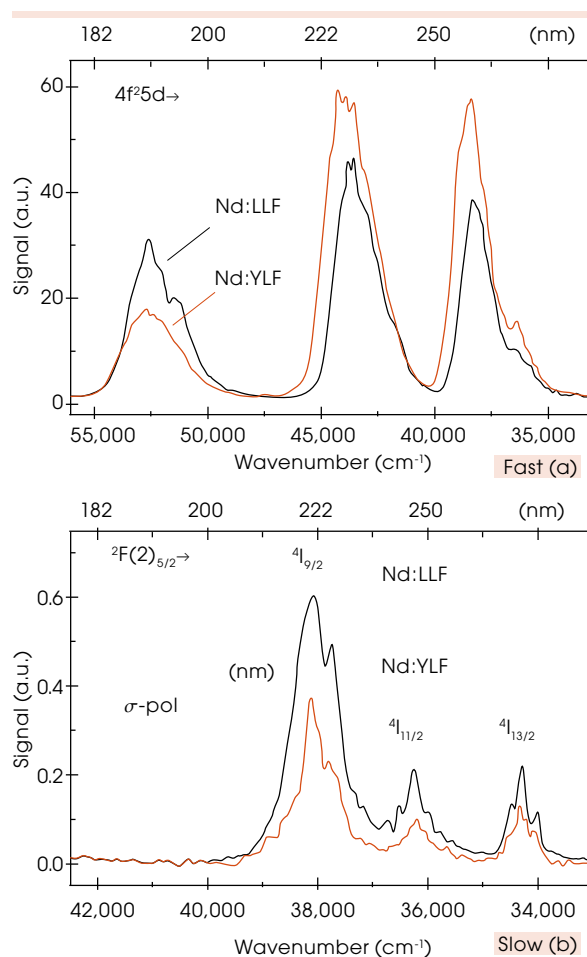
The thermal lens effect produces a strong signal decreasing and a bad signal-noise ratio, which can disguise the UV emission signal. A non-divergent beam and energies ranging from 20 to 200  $\mu\text{J}$  can be used to improve UV fluorescence performance. All the absorptions and measurements were performed with the samples at 300 Kelvin (K).

### 3 Results and discussions

The frequency doubled Nd:YAG Q-switched laser operating at 532 nm with a repetition rate of 10 hertz (Hz) was used in all the investigations of UV fluorescences. The spectrum of fast emission is due to  $4f^25d \rightarrow 4f^3$  parity allowed dipole transitions. Graphic 1a shows the emission spectrum of the fast transition showing three main emission bands downwards to  $^4I_{9/2}$  at 185 nm,  $^2H(2)_{9/2}$  at 230 nm and  $^2H(2)_{11/2}$  and  $^2G(1)_{7/2}$  at 265 nm. The  $4f^25d$  emissions were spectrally separated from the  $4f^3$  ones using a time resolved spectroscopy where the luminescence signal was integrated in the boxcar integrator within a narrow gate 2 ns positioned with a time delay of 40 ns for the fast emissions or 5 microseconds ( $\mu\text{s}$ ) for the slow ones. The  $4f^3$  configuration contributes for the UV emission due to a two photon excitation process. Graphic 1b shows the UV emission spectrum of the slow transitions starting from  $^2F(2)_{5/2}$  state pumped by two photons absorption at 532 nm. The main emission bands exhibited in Graphic 1b were produced by the following downward transitions to  $^4I_{9/2}$  at 262.3 nm (1/38,127 centimeters (cm) or 38,127  $\text{cm}^{-1}$ ),  $^4I_{11/2}$  at 276.2 nm (36,206  $\text{cm}^{-1}$ ),  $^4I_{13/2}$  at 291.3

nm (34,325  $\text{cm}^{-1}$ ) and  $^4I_{15/2}$  at 310 nm (32,258  $\text{cm}^{-1}$ ) in YLF (KOLLIA et al., 1998).

The  $4f^25d \rightarrow 4f^3$  UV emission bands exhibited in Graphic 1a showed that the band structure is similar for both YLF and LLF crystals. However, a strong shift of main emission peaks towards the lowest energy side was observed in LLF in comparison with the peak positions observed in YLF crystal. The fast UV emission bands have shown a peak shift of 421, 395 and 391  $\text{cm}^{-1}$  respectively for the 185, 230 and 265 nm emission bands. The mean energy shift of 402  $\text{cm}^{-1}$  was determined for the bottom of the  $4f^25d$  electronic configuration



**Graphic 1: UV emission bands of Nd<sup>3+</sup> in both YLF and LLF crystals excited at 532 nm by pulsed laser with 120 millijoules (mJ) of energy at 10 Hz and 4 ns of time duration**

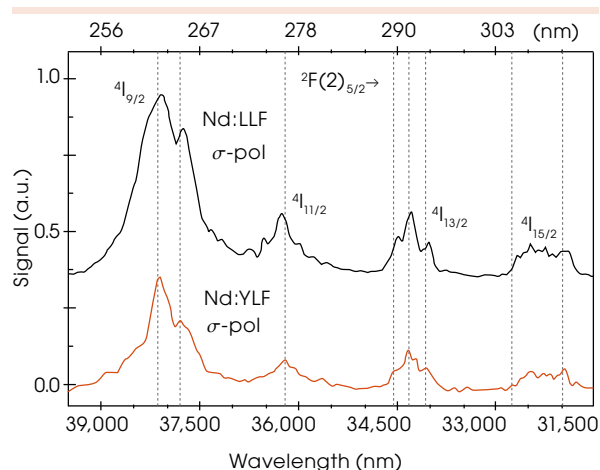
Source: The authors.

of  $\text{Nd}^{3+}$  due to the crystal lattice change from YLF to LLF. That observed emission shift is justified by the strongest electric field sensed by  $\text{Nd}^{3+}$  ions in LLF lattice and is consistent with the lattice parameter decreasing observed for this crystal where the c-axis is reduced by 1.78% in respect to YLF (RANIERI, 2000).

Graphic 1a shows the fast emission spectrum bands Graphic 1b the slow components of the UV emission ( $^2\text{F}(2)_{5/2} \rightarrow ^4\text{I}_{9/2}, ^4\text{I}_{11/2}, ^4\text{I}_{13/2}$ ).

Also the effective ionic radius of  $\text{Lu}^{3+}$  is 10.4% smaller than the effective ionic radius of  $\text{Nd}^{3+}$  in fluorides for coordination number eight (JIA, 1991).  $\text{Nd}^{3+}$  ion must be very tight when substituting the  $\text{Lu}^{3+}$  in the LLF lattice. On the other hand, the up conversion emissions from  $4f^3$  configurations have exhibited a rather small blue or red shift due to the local field increasing in LLF. See Graphics 2, 3a, and 3b, which exhibit the s-polarized emission spectra from  $^2\text{F}(2)_{5/2}$  excited state of  $\text{Nd}^{3+}$  after the laser excitation at 532 nm. For example, the  $^2\text{F}(2)_{5/2} \rightarrow ^4\text{I}_{9/2}$  emission peak at 262.3 nm exhibited a mean peak shift of  $90 \text{ cm}^{-1}$  (Graphic 2). It is observed a gradual decrease of the energy shift from the  $^2\text{F}(2)_{5/2}$  state as the energy of the transition decreases. Looking carefully the spectrum shown in the Graphics 2, 3a, and 3b, one see that the emission bands are spectrally larger in LLF than in YLF host. This effect is more evident for the  $^2\text{F}(2)_{5/2} \rightarrow ^4\text{I}_{9/2}$  and  $^2\text{F}(2)_{5/2} \rightarrow ^4\text{F}_{5/2}$  emissions where the splitting between main peaks are larger in LLF than is observed in YLF crystal.

The spectroscopic technique and method employed in this work allowed the spectral discrimination of the fast UV and slow UV-VIS (from ultraviolet to visible region) luminescence of excited  $\text{Nd}^{3+}$  ions in both YLF and LLF crystals allowing the determination the energy shift of several emissions of  $\text{Nd}^{3+}$  observing the change of emission peak energy of many transitions from  $^2\text{F}(2)_{5/2}$  level



**Graphic 2: UV s-polarized emissions from  $^2\text{F}(2)_{5/2}$  excited state to  $^4\text{I}_{9/2}, ^4\text{I}_{11/2}, ^4\text{I}_{13/2}$  and  $^4\text{I}_{15/2}$  states**

Source: The authors.

in both crystals. The energy shift  $\Delta E$  observed in the emission bands is given by

$$\Delta E_{\text{emiss}} = E_{\text{YLF}} - E_{\text{LLF}} \quad (1)$$

where  $E$  is the peak energy of the emission band. By defining  $\delta$  as the mean energy shift induced in the position of the  $^2\text{F}(2)_{5/2}$  fluorescent levels investigated and  $\chi$  the mean shift correspondent to the lower level reached in the emission transition.

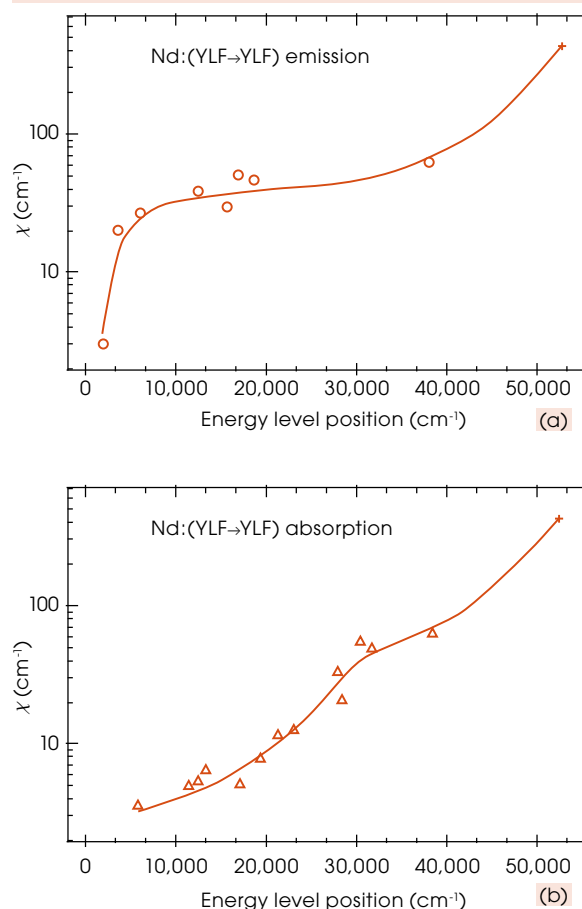
By this consideration we can write that

$$\Delta E_{\text{emiss}} = \delta - \chi \quad (2)$$

By assuming that the  $^4\text{I}_{9/2}$  ground state has no energy shift ( $\chi = 0$ ) under crystal host change (YLF  $\rightarrow$  LLF) one obtains that  $\delta$  is equal to  $90 \text{ cm}^{-1}$  after observing the energy shift of  $^2\text{F}(2)_{5/2} \rightarrow ^4\text{I}_{9/2}$  emission. So, using that  $\delta = 90 \text{ cm}^{-1}$  in Equation 2, we estimated the  $\chi$  value for several relaxed excited states of  $\text{Nd}^{3+}$  ion. In the case of absorption,  $\delta$  is equal to  $\Delta E$  because the transition always starts from  $^4\text{I}_{9/2}$  ground state which has  $\chi = 0$ . Graphic 3 shows the module of the energy level shift as function of the energy position of the excited

state of  $\text{Nd}^{3+}$  in the YLF in a semi-logarithmic scale obtained from the emission and absorption measurements.

It is seen a non-linear correlation between  $\chi$  and the energy level position when going from the lowest to the  ${}^2\text{F}(2)_{5/2}$  highest excited state of  $4f^3$  configuration and to the bottom of  $4f^25d$  configuration of  $52,567 \text{ cm}^{-1}$ . Three distinct stages are seen in Graphic 3a. The first stage shows an accentuated increasing of  $\chi$  with the increasing energy of the excited state up to  ${}^4\text{I}_{13/2}$  level. The second stage exhibits a non-pronounced increase of  $\chi$  with the energy level increase to  ${}^4\text{F}_{5/2}$  level. The third stage begins with the  ${}^2\text{F}(2)_{5/2}$  level near the charge transfer state position (located around  $40,200 \text{ cm}^{-1}$  for Nd in YLF [JIA, 1991]) exhibiting a strong  $\chi$  increasing from  $\sim 90$  to  $402 \text{ cm}^{-1}$  ( $4f^25d$  configuration). Graphic 3b shows the behavior of  $\chi$  derived from absorption measurements. It is seen a non linear dependence of  $\chi$  as function of E, exhibiting a little bump near  $E \sim 30,000 \text{ cm}^{-1}$ . This different behavior obtained from module absorption measurement is probably produced by the differences existing between the configuration of the upper excited level reached in the absorption (upward transition) and the relaxed excited state involved in the experiment. Downward transition (emission) occurs always from the relaxed excited state, which has a different equilibrium position with the neighboring ions in the lattice compared with the excited state reached in the absorption process (upward transition). The third stage begins with the  ${}^2\text{F}(2)_{5/2}$  level near the charge transfer state position (located around  $40,200 \text{ cm}^{-1}$  for Nd in YLF [JIA, 1991]) exhibiting a strong  $\chi$  increasing from  $\sim 90$  to  $402 \text{ cm}^{-1}$  ( $4f^25d$  configuration). Graphic 3b shows the behavior of  $\chi$  derived from absorption measurements. It is seen a non linear dependence of  $\chi$  as function of E, exhibiting a little bump near  $E \sim 30,000 \text{ cm}^{-1}$ .



**Graphic 3: Shows the energy shift ( $\chi$ ) induced in  $\text{Nd}^{3+}$  as function of the energy level position in YLF crystal due to the host lattice change from YLF to LLF**

Source: The authors.

This different behavior obtained from module absorption measurement is probably produced by the differences existing between the configuration of the upper excited level reached in the absorption (upward transition) and the relaxed excited state involved in the experiment. Downward transition (emission) occurs always from the relaxed excited state, which has a different equilibrium position with the neighboring ions in the lattice compared with the excited state reached in the absorption process (upward transition). The growth of  $\chi$  as the energy of the excited energy level increasing shows that the electronic shield of  $4f^3$  configurations of  $\text{Nd}^{3+}$  suffers a screening effect as the energy level



approximates to the bottom of  $4f^25d$  configuration. Within this configuration, the screening effect must be maximized. Our result is consistent to this expectation. In further steps we intend to investigate another pumping mechanism of excitation in order to improve the UV luminescence and to increase the signal-noise ratio. It will be used the OPO-VIS (optical parametric oscillator tuned at visible region) tunable laser.

## 4 Final considerations

The Nd:LLF crystal shows a three photons multistep absorption at 532 nm allowing the population of a  $4f^25d$  configuration similar to the previous excitation mechanism observed in Nd-doped YLF crystal (KOLLIA et al., 1998). This observation validates the use of LLF crystal as a promising system for UV laser operation near 265 nm. The spectral discrimination of the fast UV emission from  $4f^25d$  configuration to the slow UV emission component, allowed us to better understand the effect of the crystalline field increasing in Nd-doped fluoride crystal of YLF type.

## Notes

- 1 N. Ed.: Texto baseado em trabalho originalmente apresentado no 25º Encontro Nacional de Física de Matéria Condensada (ENFMC), em Caxambu (MG), em 2002; posteriormente publicado em *Annals of Optics*, sob organização da Sociedade Brasileira de Física (SBF).
- 2 The authors thank the Coordenação de Aperfeiçoamento de Pessoal de Nível Superior (Capes) and Fundação de Amparo à Pesquisa do Estado de São Paulo (Fapesp) (95/4166-0 and 00/10986-0, respectively) which have supported this work.
- 3 See chapter 8.
- 4 See chapter 10.

## References

- CEFALAS, A. C. et al. On the development of new VUV and UV solid-state laser sources for photochemical applications. *Laser Chemistry*, Abingdon, vol. 13, no. 2, pp. 143-150, 1993.
- EHRlich, D. J.; MOULTON, P. F.; OSGOOD JUNIOR, R. M. Ultraviolet solid-state Ce-YLF laser at 325 nm. *Optics Letters*, Washington, vol. 4, n. 6, pp. 184-186, 1979.
- GUYOT, Y.; GUY, S.; JOUBERT, M-F. Efficient  $4f^3$  ( $4f^3/2$ )  $\rightarrow$   $4f^25d$  excited state absorption in  $Nd^{3+}$  doped fluoride crystals. *Journal of Alloys and Compounds*, Amsterdam, vol. 323-324, pp. 722-725, 2001.
- JIA, Y. Q. Crystal radii and effective ionic radii of the rare earth ions. *Journal of Solid State Chemistry*, Amsterdam, v. 95, pp. 184-187, 1991.
- JOUBERT, M-F. et al. Fluoride crystals and high lying excited states of rare earth ions. *Journal of Fluorine Chemistry*, Amsterdam, vol. 107, no. 2, pp. 235-240, 2001.
- KARIMOV, D. N. et al. VUV spectroscopy of a new fluoride system NaF-(Er, Y)F-3. *Optical Materials*, Amsterdam, vol. 16, no. 4, pp. 437-444, 2001.
- KOLLIA, Z. et al. On the  $4f^25d \rightarrow 4f^3$  interconfigurational transitions of  $Nd^{3+}$  ions in  $K_2YF_5$  and  $LiYF_4$  crystal hosts. *Optics Communications*, Amsterdam, vol. 149, no. 4-6, pp. 386-392, 1998.
- MAKHOV, V. N. et al. VUV emission of rare-earth ions doped into fluoride crystals. *Journal of Luminescence*, Amsterdam, vol. 87, no. 9, pp. 1,005-1,007, 2000.
- POWELL, C. R. (Ed.). *Physics of solid-state laser materials*. 1. ed. New York: AIP Press: 1998.
- THOGERSEN, J.; GILL, J. D.; HAUGEN, H. K. Stepwise multiphoton excitation of the  $4f^25d$  configuration in  $Nd^{3+}$ :YLF. *Optics Communications*, Amsterdam, vol. 132, pp. 83-88, 1996.
- VENIKOUAS, G. E. et al. Spectroscopy of  $Y_3Al_5O_{12}$ :  $Nd^{3+}$  under high-power, picosecond-pulse excitation. *Physical Review B*, Ridge, vol. 30, no. 5, pp. 2,401-2,409, 1984.
- WEGH, R. T.; MEIJERINK, A.; LAMMINMAKI, R-J. Extending Dieke's diagram. *Journal of Luminescence*, Amsterdam, vol. 87-89, pp. 1,002-1,004, 2000.

Recebido em: 19 abr. 2006 / aprovado em: 20 jun. 2006

### Para referenciar este texto

LIBRANTZ, A. F. H. et al. Investigation of energy shift of  $4f^3$  and  $4f^25d$  levels in Nd-doped YLF and LLF crystals. *Exacta*, São Paulo, v. 4, n. 1, p. 123-128, jan./jun. 2006.